ELSEVIER

Journal of Nuclear Materials 307–311 (2002) 1178–1182

journal of nuclear materials

www.elsevier.com/locate/jnucmat

Analysis of possible deformation mechanisms in helium–ion irradiated SiC

S. Nogami [a,*], S. Ohtsuka [a], M.B. Toloczko [b], A. Hasegawa [a], K. Abe [a]

[a] *Department of Quantum Science and Energy Engineering, Tohoku University, Aramaki-aza-Aoba 01, Aoba-ku, Sendai, Miyagi 980-8579, Japan*

[b] *Pacific Northwest National Laboratory, P.O. Box 999, Richland, WA 99352, USA*

Abstract

Possible modes of accommodating deformation during physically constrained swelling of SiC during He–ion irradiation ($\sim 2 \times 10^{22}$ He/m^2 below 200 °C) were studied using finite element modeling. When accommodating deformation occurs only by elastic deformation, calculated internal stresses are much higher than the fracture stress for SiC. On the other hand, stresses below the fracture stress result when allowing irradiation-enhanced creep (IEC) to act as an additional accommodation mechanism. For a steady-state IEC compliance coefficient for SiC equal to 6×10^{-5} MPa^{-1} dpa^{-1}, the maximum observed von Mises stress was less than the fracture stress of the material. This value for the creep compliance appears to be significantly larger than the few experimentally available measured values for crystalline SiC in the open literature.

1. Introduction

Silicon carbide (SiC) is considered to be very attractive as a structural material under high energy neutron irradiation conditions such as in a fusion reactor because of its low induced radioactivity and excellent mechanical properties at elevated temperature [1,2]. Irradiation-induced dimensional changes such as swelling are one of the characteristics that has to be assessed for SiC. To evaluate irradiation-induced swelling of SiC, a technique has been applied, which involves selectively ion-irradiating a surface by placing a mask over the sample during ion-irradiation as shown in Fig. 1 [3–7]. Many swelling regions and a non-swelling region can be simultaneously formed on a sample surface due to ion-irradiation. As a result, swelling can be evaluated by measuring the difference of the step-height between the swelling and non-swelling regions.

Extremely large swelling of β-SiC caused by helium (He) ion irradiation up to about 2×10^{22} He/m^2 below 200 °C has been shown by Ohtsuka et al. using this technique [4–6], where swelling, S, was calculated from the following formula in their work:

$$S = \Delta h / R, \quad (1)$$

where Δh and R is the step-height and the projected range of the He–ions, respectively. Other irradiation conditions in the work by Ohtsuka et al. are summarized as follows [4–6]: The projected range of the He–ions was about 4 μm. The maximum dose and dose rate were 25.6 dpa and 1.42×10^{-3} dpa/s, respectively. In the irradiated regions, a high concentration of He-bubbles in the vicinity of the projected range of He–ions and amorphization were detected by transmission electron microscopy (TEM) [4]. The exterior appearance around the swelling region was smooth with no evidence of cracking or blistering. Since SiC is a brittle material, the lack of cracking or blistering warranted an investigation of the possible accommodating deformation mechanisms in the vicinity of the irradiated region.

* Corresponding author. Tel.: +81-22 217 7924; fax: +81-22 217 7925.

E-mail address: nogami@jupiter.qse.tohoku.ac.jp (S. Nogami).

0022-3115/02/$ - see front matter © 2002 Elsevier Science B.V. All rights reserved.
PII: S0022-3115(02)01058-9

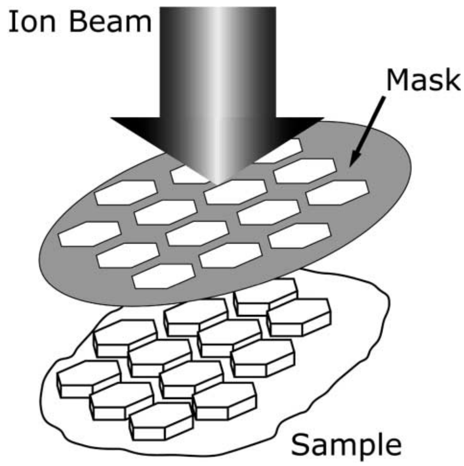

Fig. 1. Schematic illustration of the technique involving selectively ion-irradiating a surface by placing a mask over the sample during ion-irradiation.

The objective of this work is to use finite element modeling (FEM) to simulate the experimental study of He–ion irradiated SiC by Ohsuka et al. [4–6], and, to examine why neither cracking nor blistering occurred during their experiments. Possible accommodating deformation mechanisms include elasticity and irradiation-enhanced creep (IEC). Plastic deformation by dislocation motion at temperatures below 200 °C was not considered in this study for two reasons. First, dislocation motion has only been observed in SiC when loaded in compression such as in the indentation test [8], whereas the major stress along the boundary between the irradiated and unirradiated region in the work by Ohtsuka et al. is tensile. Second, much of the region where the deformation occurred became amorphous during irradiation, and in the previous study [4], no dislocations were detected by TEM after amorphization.

2. Method of analysis

The FEM analysis was carried out using the MARC FEM program. Fig. 2 shows a model for this analysis. Axisymmetric quadrilateral elements symmetrical about the x-axis (32 μm ∅ × 30 μm t) that describe just one irradiated region were used. Displacement of the nodes in the bottom region ($x = 30$ μm) and the nodes in the side region ($r = 32$ μm) were fixed in the x-direction and r-direction, respectively. The irradiated area had a circular shape (20 μm ∅) in this analysis. In the study, by Ohtsuka et al. the shapes were hexagonal and square [4–6]. Based on TEM observations in the previous work [4], the depths of the amorphous-induced swelling and the He-bubble swelling regions (grey and black zones in Fig. 2, respectively) were determined to be 0–4.5 μm and 3.5–4.0 μm, respectively.

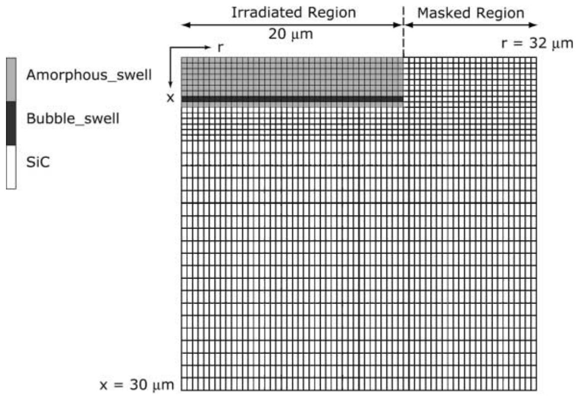

Fig. 2. A model for the FEM analysis. Axisymmetric quadrilateral elements symmetrical about the x-axis (32 μm ∅ × 30 μm t) that describe just one irradiated region were used.

Fig. 3 shows a schematic illustration of cavity growth during ion-irradiation in which swelling induced by amorphization was assumed to be isotropic, while swelling induced by He-bubble formation was orthotropic. H_0 and L_0 denote the thickness and width of a region with cavities perpendicular to the ion-direction at time of t_0, respectively. $H_0 + \Delta H$ and $L_0 + \Delta L$ denote the values at time of $t_0 + \Delta t$. The length strain $\Delta L/L_0$ is very small compared with the height strain $\Delta H/H_0$ because cavity growth was due to aggregation of a thin layer of small cavities at H_0. For the purposes of the present study, the length change of the bubble swelling region, ΔL, was set equal to zero. This means that the bubble-swelling region could grow uniformly only in the x-direction as defined by the irradiated region in the FEM model.

Simulation of the swelling in SiC induced by amorphization and He-bubble formation was performed by using thermal expansion routines in the FEM program. Assigning an artificial thermal expansion coefficient to the elements which are designated to swell and then heating the elements over an arbitrary temperature interval will cause an element to expand. The fact that the

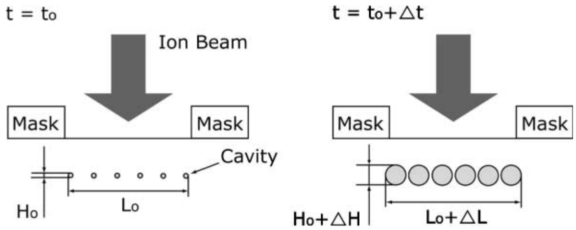

Fig. 3. Schematic illustration of cavity growth during ion-irradiation when the sample is masked.

elements are heated is only incidental to the method and has no effect on actual assigned mechanical properties of elements except to cause them to expand. In this study, the temperature was set initially at 0 K and then incrementally increased to 1 K. By equating the total thermal expansion strain over a 1 K temperature change to the total linear swelling strain, the artificial coefficient of thermal expansion, α, for the FEM analysis is calculated from the following formula:

$$\alpha \approx (1/3)S. \quad (2)$$

Swelling, S, was calculated to be about 20% for the amorphous swelling and about 300% for the bubble swelling based on the previous studies [3–6]. Using Eq. (2), the artificial thermal expansion rates, α, were determined to be 0.07 K^{-1} and 1.00 K^{-1}, respectively.

Other material properties used in this model are summarized as follows: The Young's modulus in the unirradiated SiC was the actual value (490 GPa) for β-SiC_{CVD} fabricated by Mitsui Engineering and Shipbuilding Co. Ltd. [9]; the Young's modulus in the irradiated SiC changed from 490 to 290 GPa, that is the experimental value for the neutron-irradiated amorphised SiC [10]; and Poisson's ratio was 0.2 in the whole region.

3. Results and discussion

3.1. Elastic deformation analysis

Elastic deformation analysis was performed using the FEM mesh shown in Fig. 2. Fig. 4 shows the distribution of the calculated equivalent von Mises stress after 18 000 s (the irradiation time in the previous research [4–6]). Peak stresses (~22 GPa at the center of the irradiated region) were much higher than the fracture stresses (588 MPa in tensile and 784 MPa in bending for SiC [9]), especially at the boundary between the swelling and non-swelling region. This result suggests that elastic deformation alone should lead to cracking or blistering. However, cracking and blistering were not observed in the previous experiments [4–6]. Therefore, there must be an additional deformation mechanism operating.

3.2. Combined creep and elastic deformation analysis

IEC was assumed to be the major additional deformation mechanism in this study. Vacancies are immobile at temperatures below 200 °C leaving interstitial migration as the most likely mechanism for IEC in SiC at temperatures covered in this study. In this situation, IEC should be roughly proportional to the product of the interstitial concentration and the interstitial mobility. According to the Rutherford backscattering spectrometry-channeling [11,12], the isochronal recovery of the silicon (Si) disorder on the Si sublattice for 6H–SiC irradiated with He^{+}, Si^{+} and Au^{+}-ions occurred below about 200 °C. This result suggests that Si interstitials may be mobile below about 200 °C. However, it is known that the displacement energy for C in SiC is lower than that for Si in SiC (20 eV versus ~40 eV) [13] which will result in a higher concentration of C interstitials. Thus, it is possible that both Si and C interstitials may be contributing to IEC in the range of temperatures covered in this study.

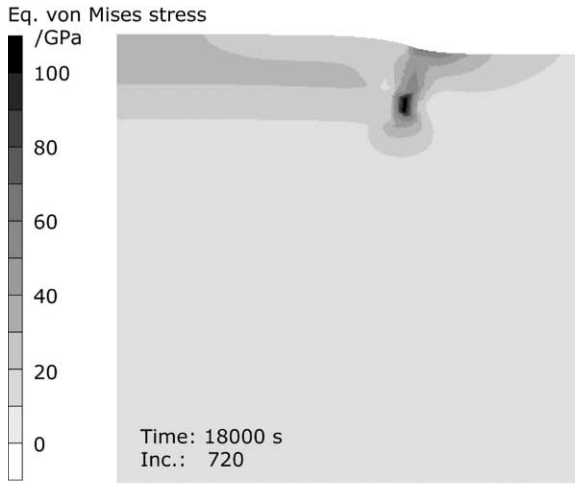

Fig. 4. The distribution of the calculated equivalent von Mises stress after 18 000 s for the elastic deformation model.

Based on an assumption of a diffusion-controlled creep mechanism, IEC was introduced into the FEM model as an additional deformation mechanism. The following simple steady-state creep model with a linear dependence on stress σ and dose Φ was used to describe the material behavior in this analysis [14–16]

$$\varepsilon_{cr} = B_0 \sigma \Phi, \quad (3)$$

where ε_{cr} and B_0 are a creep strain and IEC-compliance coefficient, respectively. However, since the FEM model is a time-based model rather than a dose-based model, the creep response of the elements is described by a time dependent equation. This equation has the form

$$\varepsilon_{cr} = A_0 \sigma t, \quad (4)$$

where A_0 and t are a creep-compliance coefficient and a time, respectively.

Fig. 5(a) and (b) shows a typical result for the creep deformation analysis and the distribution of the equivalent von Mises stress of this model after 18 000 s, respectively. The dose distribution was calculated by using the TRIM-code [4–6]. Selected values of B_0 are also shown. Significant stress relaxation was achieved when creep deformation was included. The maximum stress

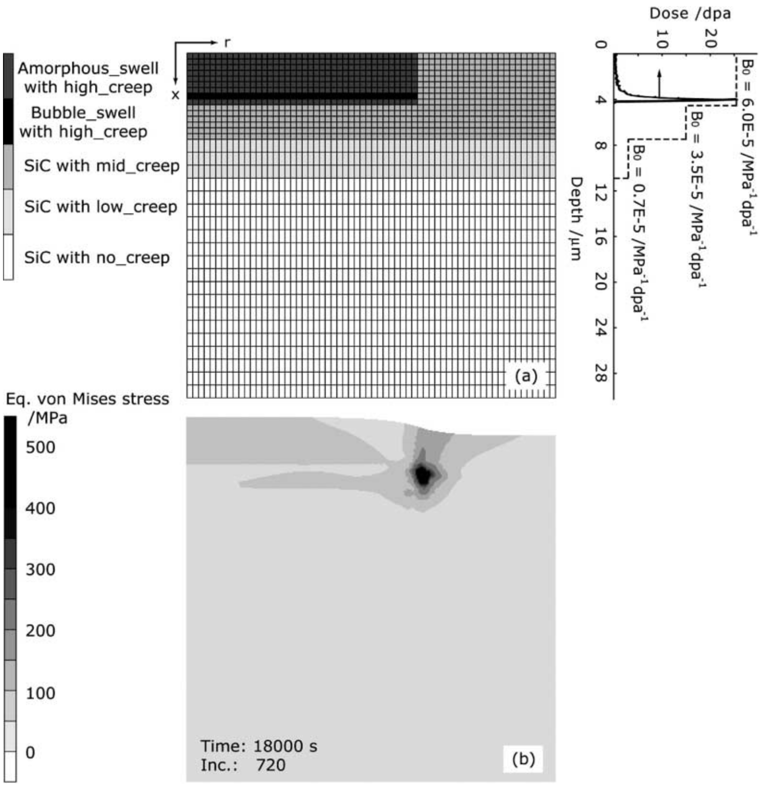

Fig. 5. (a) A typical result for the creep deformation analysis in this study, and (b) the distribution of the equivalent von Mises stress after 18 000 s for the model. Calculated dose distribution and selected values of B_0 in each region are also shown.

was restricted never to exceed about 500 MPa in this calculation. The results show that the stress in the x-direction at the center of the irradiated region ($r = 0$ μm and $x = 4$ μm) was reduced from ~8.8 GPa in the elastic analysis to ~43 MPa in the creep analysis. The selected values for B_0 $(= A_0/(\Phi/t))$ in each region were calculated by setting Eq. (3) and 4 equal to each other, where $\Phi/t = 1.42 \times 10^{-3}$ dpa/s (25.6 dpa/18 000 s) from the previous studies [4–6] was used. The maximum value for B_0 for SiC in this study (6×10^{-5} MPa^{-1} dpa^{-1}) was somewhat larger than the few experimentally available measured values for crystalline SiC in the open literature (about 2×10^{-6} MPa^{-1} dpa^{-1}) [15,16]. The maximum step-height estimated using this creep model was about 1.7 μm at the center of the bump (the node in $r = x = 0$ μm at $t = 0$ s), while a value of about 1.6 μm was measured in the previous works [4–6].

4. Summary

Deformation mechanisms accompanied by He–ion irradiation-induced swelling of β-SiC with a mask-technique were studied using FEM analysis. The following results were obtained:

1. When elasticity was the only deformation mechanism, internal stresses at the boundary between the irradiated and the unirradiated regions were calculated to be much higher than the fracture stress of β-SiC.
2. When deformation was permitted to occur by both elasticity and irradiation-creep, the stresses were much lower. Depending on the value used for the IEC-compliance coefficient, the calculated stresses could be lower than the fracture stress.
3. The deformation region transformed from crystalline to amorphous during irradiation, and the calculated IEC-compliance coefficient for this material ($\leqslant 6 \times 10^{-5}$ MPa^{-1} dpa^{-1}) was somewhat larger than the few experimentally available measured values for crystalline SiC in the open literature.

5. Conclusions

Elastic deformation alone cannot provide the deformation necessary to keep the stresses below the fracture stress in this study. With a sufficiently large IEC-compliance coefficient, IEC can provide the deformation necessary to keep the stresses below the fracture stress. However, the large value for the IEC-compliance coefficient needed to keep the stresses below the fracture stress suggests that further study of deformation in this unique experiment is needed.

Acknowledgements

The authors are grateful to the staff of Information Synergy Center at Tohoku University for maintaining their super computer and work stations. This work was partly supported by the JUPITER (Japan–USA Program of Irradiation Testing for Fusion Research) program. This work was also partly supported by the Japan Nuclear Cycle Development Institute.

References

[1] A. Hasegawa, A. Kohyama, R.H. Jones, L.L. Snead, B. Riccardi, J. Nucl. Mater. 283–287 (2000) 128.
[2] L.H. Rovner, G.R. Hopkins, Nucl. Tech. 29 (1976) 274.
[3] S. Nogami, S. Ohtsuka, M.B. Toloczko, A. Hasegawa, K. Abe, in: Proceedings of the 4th Pacific Rim International Conference on Advanced Materials and Processing, 2001, p. 1367.
[4] S. Ohtsuka, A. Hasegawa, M. Satou, K. Abe, in press.
[5] S. Ohtsuka, A. Hasegawa, M. Satou, K. Abe, in: Proceedings of the 1998 International Conferene on Ion Implantation Technology, Ion Implantation Technology-98, 1999, p. 779.
[6] S. Ohtsuka, A. Hasegawa, M. Satou, K. Abe, in: Proceedings of the International Symposium on Environmental-Conscious Innovate Materials Processing with Advanced Energy Sources, 1998, p. 424.
[7] H. Kishimoto, Y. Katoh, A. Kohyama, M. Ando, in: Proceedings of the 2nd Asian–Australasian Conference on Composite Materials, II, 2000, p. 733.
[8] W.C. Oliver, R. Hutchings, J.B. Pethica, Microindentation Techniques in Material Science and Engineering, P.J. Blau, B.R. Lawn (Eds.), ASTM STP 889, ASTM, Philadelphia, PA, 1986, p. 90.
[9] Y. Chinose et al., Amorphous and Crystalline Silicon Carbide and Related Materials, M.M. Rahman, C.Y.W. Yang, G.L. Harris (Eds.), Springer Proceedings in Physics 43, Springer-Verlag, 1989, p. 198.
[10] L.L. Snead, J.C. Hay, J. Nucl. Mater. 273 (1999) 213.
[11] W.J. Weber, W. Jiang, S. Thevuthasan, Nucl. Instrum. and Meth. B 166–167 (2000) 410.
[12] F. Gao, W.J. Weber, W. Jiang, Phys. Rev. B 63 (2001) 214106.
[13] S.J. Zinkle, C. Kinoshita, J. Nucl. Mater. 251 (1997) 200.
[14] C.A. Lewinsohn, M.L. Hamilton, G.E. Youngblood, R.H. Jones, F.A. Garner, S.L. Hecht, A. Kohyama, J. Nucl. Mater. 253 (1998) 36.
[15] R. Scholz, G.E. Youngblood, J. Nucl. Mater. 283–287 (2000) 372.
[16] R.J. Price, Nucl. Technol. 35 (1977) 320.